Rotational spectra, structures, and dynamics of small Ar m –(H2O) n clusters: The Ar2–H2O trimer

E. Arunan, C. E. Dykstra, T. Emilsson, and H. S. Gutowsky

Citation: The Journal of Chemical Physics **105**, 8495 (1996); doi: 10.1063/1.472611
View online: http://dx.doi.org/10.1063/1.472611
View Table of Contents: http://scitation.aip.org/content/aip/journal/jcp/105/19?ver=pdfcov
Published by the AIP Publishing

Rotational spectra, structures, and dynamics of small $Ar_m-(H_2O)_n$ clusters: The Ar_2-H_2O trimer

E. Arunan
Department of Chemistry, Indian Institute of Technology, Kanpur, 208 016 India

C. E. Dykstra
Department of Chemistry, Indiana University-Purdue University Indianapolis, Indianapolis, Indiana 46202

T. Emilsson and H. S. Gutowsky
Noyes Chemical Laboratory, University of Illinois, Urbana, Illinois 61801

(Received 25 July 1996; accepted 12 August 1996)

Rotational spectra have been observed for the Ar_2-H_2O trimer and several of its isotopomers with the Balle/Flygare pulsed nozzle, Fourier transform microwave spectrometer. Analysis gives a planar T-shaped structure with C_{2v} symmetry and the bidentate protons pointed at the argons. Two sets of asymmetric top transitions were found for the species with H_2O, D_2O, or $H_2{}^{18}O$. Several lines of evidence support assigning them to internal rotor states of the water, the upper set to $\Sigma(0_{00})$ and the lower to $\Sigma(1_{01})$ as in the $Ar-H_2O$ dimer. Support includes: Hyperfine interaction constants which differ for the two states of water; Systematic aspects of the rotational constants such as *B*'s that are little affected by isotopic substitution; and MMC calculations which indicate the importance of rovibrational coupling. The Ar–Ar distance for the $\Sigma(0_{00})$ state of the trimer is estimated to be 3.822 Å and the center of mass (Ar_2) to center of mass (H_2O) distance to be 3.173 Å. An intriguing result is finding the hyperfine interaction constants of the water in the trimer to be very nearly the same as those reported earlier for the dimer. This shows the two dynamic states of the water are the same in the dimer and trimer, as is the average projection of the water C_2 axis onto the inertial frame. [S0021-9606(96)00843-4]

INTRODUCTION

The structure of the weakly bonded $Ar-H_2O$ dimer has been characterized in considerable detail.[1–4] More recently a preliminary account has been given[5] of the structural dynamics of the four next larger heteromolecular Ar/H_2O clusters as seen by rotational spectroscopy. Such studies are of interest because the Ar/H_2O systems is a prototype for the hydrophobic interactions which are significant in a variety of areas ranging from biological systems to partition separations.[6–9] Our results thus far suggest that the small Ar/H_2O clusters have structures analogous to the closest packing of spheres. This is perhaps not surprising because the argon is spherical, the H_2O is nearly so, and they are of comparable size. Moreover the effective shape of the H_2O is an average over the dynamics, and the PES (potential energy surface) of the clusters is isotropic enough for internal rotation and tunneling to make the H_2O appear more nearly spherical in the clusters.

We find the particular case of Ar_2-H_2O to be an asymmetric top with a T-shaped structure and C_{2v} geometry. Its properties are very similar to those of Ar_2-HF, the first trimeric complex[10] to be characterized by FTMW (Fourier transform microwave) spectroscopy.[11–13] Ar_2-H_2O is noteworthy in having two sets of transitions separated by ~100 MHz (for $J \lesssim 3$). For the parent isotopic species the upper set consists of sharp singlets while the lower set has weak hyperfine structure or unresolved broadening in the low *J* transitions. The sets are assigned respectively to the singlet (*para*, $I_H=0$) and triplet (*ortho*, $I_H=1$) spin states of H_2O. However, the spin states may be combined with either internal rotor or tunneling states depending primarily on the anisotropy of the PES governing the dynamics of the H_2O. This question was not addressed in the preliminary account but is given major attention here.

Another feature treated here is the equilibrium orientation of the H_2O with respect to the Ar_2. In $Ar-H_2O$ one of the hydrogens is significantly closer to the Ar than is the other.[3] In contrast, Ar_2-H_2O allows the bidentate character of H_2O to express itself (Fig. 1). Yet the C_{2v} symmetry shown is not unique. The H_2O could be rotated from the configuration shown. Or it could be a case of pseudo symmetry generated by the dynamic state of the H_2O. The choices among these options were aided by MMC (molecular mechanics for clusters)[14] calculations of the PES and its anisotropy.

EXPERIMENT

The rotational transitions of the trimer were measured with the Illinois Balle/Flygare pulsed nozzle FTMW spectrometer.[11,12] Its modification and operation have been described in detail earlier.[13] The Ar_2-H_2O and $-D_2O$ trimers were formed by supersonic expansion of argon (Liquid Air) about 10% of which had been bubbled through H_2O or D_2O (Sigma) kept at ambient conditions. Ordinarily the backing pressure was 0.75 atm. The diameter of the 900 series valve (General Valve) was 1 mm. The frequencies reported for well resolved transitions typically have standard deviations of 0.5 kHz or less.

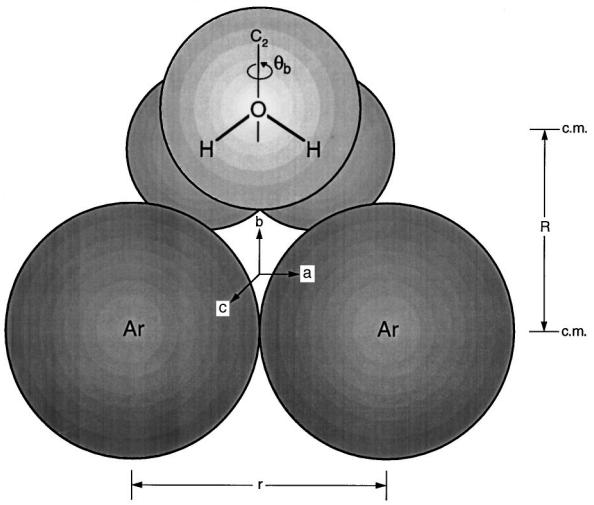

FIG. 1. A schematic view of the planar C_{2v} equilibrium structure found by MMC calculations for Ar_2–H_2O. The circles represent the atomic van der Waals radii.

EXPERIMENTAL RESULTS

Transitions and rotational constants

The search for Ar_2–H_2O was prompted in part by our expectation that the structures of the Ar_m–H_2O species would be quite similar to those reported earlier[10,15] for Ar_m–HF, and thereby readily found. This proved to be the case with Ar_2–H_2O except for the splitting by ~100 MHz of its transitions into two sets. For example, the $0_{00}\rightarrow 1_{11}$ asymmetric top transition of Ar_2–HF is at 4737 MHz while Ar_2–H_2O has transitions at 4512.5 and 4601.6 MHz. The search and assignment were also facilitated by the expected T-shaped structure for which the B rotational constant is very close to that of free Ar_2, 1733 MHz.[16] The two sets of transitions observed for Ar_2–H_2O are listed in Table I, with 26 and 34 entries for the lower and upper frequency sets, respectively. The perdeuterated species Ar_2–D_2O was also examined, with similar less extensive results given in Table II for its two sets of transitions (23 and 25 entries).

Inspection of Tables I and II shows that all of the (b-dipole) transitions found are between $J_{K-,K+}$ levels one of which has K_{-+} even–even (ee) and the other odd–odd (oo). None were found between oe and eo levels even though an asymmetric top without a symmetry axis has as many oe and eo levels as oo and ee. This absence of oe and eo levels is attributable to a twofold axis of symmetry interchanging identical spin zero nuclei (^{40}Ar).[10] Accordingly the trimer is T shaped, having C_{2v} symmetry with the b-inertial axis connecting the Ar_2 center of mass (c.m.) to the c.m. of H_2O or D_2O (Fig. 1).

The transitions at higher frequency in Tables I and II are sharp singlets for all four sets, as expected for small or absent hf interactions. However, those at lower frequency in the lower set of Ar_2–H_2O and in both sets of Ar_2–D_2O transitions showed small hfs or unresolved broadening. Some details are given for them in the next section. In their case the line centers listed were visually estimated. The frequencies of each set were fitted to the Hamiltonian for the distorted asymmetric rotor,[17] using the Watson S reduction.[18] The residues of the fits are included in Tables I and II. Their standard deviations range from 2 to 5 kHz but the sextic distortion terms, H_{jk}, H_{kj}, and H_k, are required to attain fits that good. Even so some of the residues, especially those for the lower set of Ar_2–D_2O, are 10 kHz or so, large enough to show the presence of neglected rovibrational interactions.

TABLE I. The two sets of rotational transitions observed and fitted for the triplet (I_H=1) and singlet (I_H=0) spin states of H_2O in Ar_2–H_2O.

	Triplet state (I_H=1)		Singlet state (I_H=0)	
Transition	Obs. freq. (MHz)	Res.[a] (kHz)	Obs. freq. (MHz)	Res. (kHz)
$0_{00}\rightarrow 1_{11}$	4 512.497	0	4 601.590	0
$2_{02}\rightarrow 2_{11}$	2 996.848	0	3 025.457	−3
$2_{11}\rightarrow 2_{20}$	5 082.734	1	5 300.602	2
$1_{11}\rightarrow 2_{02}$	3 940.886	1	3 900.786	−2
$1_{11}\rightarrow 2_{20}$	12 020.460	−6	12 226.846	−3
$3_{13}\rightarrow 3_{22}$	7 744.800	−1	7 887.389	−2
$3_{22}\rightarrow 3_{31}$	9 828.248	1	10 158.792	0
$2_{02}\rightarrow 3_{13}$	8 786.472	1	8 939.416	1
$2_{11}\rightarrow 3_{22}$	13 534.428	4	13 801.347	2
$4_{04}\rightarrow 4_{13}$	6 270.852	2	6 165.067	−1
$4_{13}\rightarrow 4_{22}$	4 896.277	1	5 028.462	−2
$4_{22}\rightarrow 4_{31}$	8 563.510	−2	8 974.336	0
$4_{31}\rightarrow 4_{40}$	13 312.156	2	13 814.871	2
$3_{13}\rightarrow 4_{04}$	9 656.035	0	9 703.917	−1
$3_{22}\rightarrow 4_{13}$	8 182.083	−1	7 981.595	1
$5_{14}\rightarrow 5_{24}$	⋯	⋯	10 758.193	5
$5_{24}\rightarrow 5_{33}$	⋯	⋯	11 023.764	−3
$5_{33}\rightarrow 5_{42}$	13 448.612	0	13 924.779	−2
$5_{42}\rightarrow 5_{51}$	17 247.266	0	17 870.034	2
$4_{04}\rightarrow 5_{15}$	12 730.529	0	12 921.699	−2
$4_{13}\rightarrow 5_{24}$	17 167.918	2	17 514.826	5
$6_{06}\rightarrow 6_{15}$	11 377.501	2	11 188.572	6
$6_{15}\rightarrow 6_{24}$	⋯	⋯	6 966.489	−1
$6_{24}\rightarrow 6_{33}$	⋯	⋯	7 635.838	0
$6_{33}\rightarrow 6_{42}$	12 283.818	−4	12 886.715	−1
$6_{42}\rightarrow 6_{51}$	⋯	⋯	17 698.137	−4
$5_{15}\rightarrow 6_{06}$	14 605.732	−1	14 759.055	−3
$5_{24}\rightarrow 6_{15}$	⋯	⋯	15 189.434	−1
$5_{33}\rightarrow 6_{24}$	11 585.030	−2	11 132.158	0
$7_{17}\rightarrow 7_{26}$	⋯	⋯	14 652.431	−5
$7_{26}\rightarrow 7_{35}$	12 965.659	−3	13 086.095	−3
$7_{35}\rightarrow 7_{44}$	13 855.893	4	14 261.942	4
$7_{44}\rightarrow 7_{53}$	⋯	⋯	17 679.134	1
$6_{06}\rightarrow 7_{17}$	17 026.687	1	17 247.804	1

[a]Residue=obs.−calc.

Less extensive studies were made of the partially deuterated Ar_2–HDO and the ^{18}O substituted Ar_2–H_2 ^{18}O. In both cases only 15–20 transitions of the upper state (not given) were observed and fitted. The results are given in Table III with those for the other species. A search was made for lower state transitions of the partially deuterated species, but it was unsuccessful as in the case of the Ar–HDO dimer.[3] Both upper and lower states were found for the ^{18}O substituted trimer. The upper state was observed in order to obtain a substitution value for R, the Ar_2 to H_2O distance. Also, as given in the next section, the ^{17}O hfs was measured in the

TABLE II. The two sets of rotational transitions observed and fitted for the antisymmetric (I_D=1) and symmetric (I_D=0,2) spin states of D_2O in Ar_2–D_2O.

	Antisym. spin state (I_D=1)		Sym. spin state (I_D=0,2)	
Transition	Obs. freq. (MHz)	Res.[a] (kHz)	Obs. freq. (MHz)	Res. (kHz)
$0_{00}\rightarrow1_{11}$	4 229.530	6	4 304.001	5
$2_{02}\rightarrow2_{11}$	2 837.711	−9	2 851.156	2
$2_{11}\rightarrow2_{20}$	4 359.918	0	4 532.704	−9
$1_{11}\rightarrow2_{02}$	4 097.981	−6	4 073.880	−7
$1_{11}\rightarrow2_{20}$	11 295.625	0	⋯	⋯
$3_{13}\rightarrow3_{22}$	7 139.654	−3	7 240.304	−5
$3_{22}\rightarrow3_{31}$	8 659.945	−2	⋯	⋯
$2_{02}\rightarrow3_{13}$	8 383.972	1	⋯	⋯
$2_{11}\rightarrow3_{22}$	12 685.915	7	12 909.102	2
$2_{20}\rightarrow3_{31}$	16 985.929	−8	17 295.579	1
$4_{04}\rightarrow4_{13}$	6 369.658	11	6 256.908	3
$4_{13}\rightarrow4_{22}$	4 451.648	−2	4 527.681	2
$4_{22}\rightarrow4_{31}$	7 219.241	9	7 552.803	2
$4_{31}\rightarrow4_{40}$	11 553.819	4	11 965.901	2
$3_{13}\rightarrow4_{04}$	9 561.147	−2	⋯	⋯
$3_{22}\rightarrow4_{13}$	8 791.146	6	⋯	⋯
$5_{15}\rightarrow5_{24}$	10 257.982	−5	⋯	⋯
$5_{24}\rightarrow5_{33}$	9 787.145	5	⋯	⋯
$5_{33}\rightarrow5_{42}$	11 785.028	−5	12 159.759	−3
$5_{42}\rightarrow5_{51}$	⋯	⋯	15 551.721	1
$4_{04}\rightarrow5_{15}$	⋯	⋯	12 465.710	−5
$4_{13}\rightarrow5_{24}$	16 182.055	−2	16 479.500	6
$6_{06}\rightarrow6_{15}$	11 458.312	0	⋯	⋯
$6_{15}\rightarrow6_{24}$	7 246.607	−1	⋯	⋯
$6_{24}\rightarrow6_{33}$	⋯	⋯	6 506.991	−2
$6_{33}\rightarrow6_{42}$	10 276.202	1	⋯	⋯
$6_{42}\rightarrow6_{51}$	⋯	⋯	15 307.884	−3
$5_{15}\rightarrow6_{06}$	⋯	⋯	14 423.751	−2
$5_{24}\rightarrow6_{15}$	⋯	⋯	15 453.873	−1
$5_{32}\rightarrow6_{25}$	⋯	⋯	12 571.890	2
$7_{17}\rightarrow7_{26}$	⋯	⋯	14 262.976	−1
$7_{26}\rightarrow7_{35}$	⋯	⋯	12 351.675	−3
$7_{35}\rightarrow7_{44}$	⋯	⋯	12 707.042	3
$7_{44}\rightarrow7_{53}$	⋯	⋯	15 364.083	1
$6_{06}\rightarrow7_{17}$	⋯	⋯	16 754.836	1

[a]Residue=obs.−calc.

$0_{00}\rightarrow1_{11}$ transitions of Ar_2–H_2 ^{17}O for comparison with that of the Ar–H_2 ^{17}O dimer.

The rotation and distortion constants obtained by fitting the six sets of transitions are given in Table III. They include the upper states of four isotopic species and the lower states of two of them. Comparison of the values reveals some modest systematic differences between lower and upper states and between H_2O and D_2O isotopic species. However, an unexpected result is the absence of any significant change in B upon deuterium substitution. The B's are virtually the same (1731 MHz) for all four upper states while the two lower states are the same but 3 MHz larger. In contrast, if Ar_2–H_2O were a ''normal'' C_{2v} molecule I_b (Ar_2–H_2O) would be given as $I_b(Ar_2)+I_b(H_2O)$ and D_2O substitution would decrease B by 7 MHz instead of having little effect. Deuterium substitution does affect A and C but in a complex manner suggested by the *positive* inertial defects of 6.8 and 3.4 μÅ^2 for lower and upper states.

Nuclear hyperfine interactions

Another unexpected feature was found in the nuclear hyperfine structure. The hfs is caused by interactions within the H_2O/D_2O which are the same in dimer and trimer. However, expression in the spectra of the interactions depends on the PES, which determines the internal dynamic state and differs for dimer and trimer. Therefore, we expected the hfs of the Ar_2–H_2O/D_2O and Ar_2–H_2 ^{17}O to be qualitatively similar but quantitatively different from that of the dimer, which was investigated earlier in detail.[3,4] So it was a surprise to find the hfs to be essentially the same for trimer and dimer but different for lower and upper states.

The spectra found for the four $0_{00}\rightarrow1_{11}$ transitions of Ar_2–H_2O/D_2O are given in Table IV for the trimer and those for the dimer are listed in Tables I–III of Ref. 4. The ^{17}O quadrupolar hfs has been reported for the Ar–H_2 ^{17}O dimer.[3] The present work includes the hfs in the $0_{00}\rightarrow1_{11}$ transitions of the Ar_2–H_2 ^{17}O trimer, listed and fitted in Table V. In fitting the lower state the small H–H magnetic dipolar inter-

TABLE III. Rotational and centrifugal distortion constants determined from rotational frequencies observed for several isotopic species and states of the Ar_2–H_2O trimer.

	Ar_2–H_2O		Ar_2–D_2O		Ar_2–HDO	Ar_2–H_2 ^{18}O
Parameter	Lower state	Upper state	Lower state	Upper state	Upper state	Upper state
A (MHz)	3 383.2472(8)	3 457.2255(8)	3 130.449 (2)	3 190.924(2)	3 321.829 (3)	3 178.8750(4)
B	1 734.6506(5)	1 731.7811(5)	1 734.137 (1)	1 731.472(1)	1 731.1607 (9)	1 731.7465(2)
C	1 129.4144(5)	1 144.5596(5)	1 099.214 (1)	1 140.609(1)	1 129.4110 (7)	1 112.0431(1)
D_1 (kHz)	−6.636(3)	−6.455(3)	−6.743 (8)	−6.568(5)	−6.498 (6)	−6.556(2)
D_2	−1.757(2)	−1.5955(7)	−1.817 (3)	−1.704(1)	−1.652 (4)	−1.742(1)
Dj	13.99(2)	15.36(2)	13.6 (1)	14.68(3)	15.12 (2)	14.871(5)
Djk	39.05(8)	31.48(5)	33.5 (2)	28.5(1)	30.2 (2)	31.56(4)
D_k	57.28(8)	96.70(6)	44.3 (4)	67.7(1)	85.4 (4)	76.4(1)
H_j (Hz)	−0.7(2)	−0.8(2)	⋯	−0.9(4)	⋯	⋯
H_{jk}	16(2)	15(1)	13 (7)	15(2)	15 (6)	30.8(8)
H_{kj}	−50(3)	−67(1)	−49 (15)	−60(2)	−82 (30)	−94(5)
H_k	30(2)	58(2)	35 (16)	50(3)	66 (20)	61(9)
trans	26	34	23	25	20	15
sd (kHz)	2.1	2.6	5.1	3.6	4.0	0.3

TABLE IV. Hyperfine structure of the $J=0_{00}\rightarrow 1_{11}$ transitions for Ar_2-H_2O/D_2O.[a]

Ar_2-H_2O				Ar_2-D_2O			
Lower state ($I_H=1$)		Upper state ($I_H=0$)		Lower state ($I_D=1$)		Upper state ($I_D=0,2$)	
$F\rightarrow F'$	Freq.	$F\rightarrow F'$	Freq.	$F\rightarrow F'$	Freq.	$F\rightarrow F'$	Freq.
1→1	4512.4880	0→1	4601.5897	1→1	4229.5004	2→2	4303.9652
1→2	2.4964			1→2	9.5254	0→1	3.9911
1→0	⋯			1→0	⋯	2→3	3.9911
						2→1	4.0115

[a]Frequencies are in MHz and $F=I+J$.

action of Table IV was neglectable. The D and ^{17}O quadrupole interaction constants determined for the various species and states are compared in Table VI.

Besides such information the hfs tells us the nuclear spin functions of the two protons in the lower and upper states of Ar_2-H_2O and of the two deuteriums in Ar_2-D_2O. This then places symmetry constraints upon the total wave functions ψ_T occupied by the H_2O/D_2O, and thereby upon its ''rotational'' behavior. The results summarized in Table VII are simplest for the magnetic dipole–dipole interaction of the protonated species.[4] In it the lower state has triplet $I_H=1$ hfs and the upper state has singlet $I_H=0$ transitions with no hfs. In other words the nuclear spin wave function ψ_{nuc} for the two protons is symmetric to their interchange for the lower state and antisymmetric for the upper state. Also the protons are spin-1/2 Fermions and their interchange requires an antisymmetric total wave function ψ_T. We designate by ψ_{ex} the as yet unknown operators exchanging the two proton and note that all components of ψ_T except ψ_{nuc} and ψ_{ex} are symmetric. Accordingly $\psi_{nuc}\psi_{ex}$ and ψ_T will be antisymmetric for the lower state of Ar_2-H_2O if ψ_{ex} is antisymmetric. Similarly ψ_T will be antisymmetric for the upper state if ψ_{ex} is symmetric.

The case of $Ar_2/Ar-D_2O$ is a bit more complex as reported for Ar_2-H_2O/D_2O.[4] The hfs is generated by nuclear quadrupole interactions of the two spin-1 deuterium nuclei. The latter are bosons for which ψ_T must be symmetric to exchange. The hfs observed for the lower state is assigned to the antisymmetric spin function ($I_D=1$) and for the upper state to the symmetric spin functions ($I_D=0,2$). The assignment in combination with the requirement that ψ_T be symmetric to deuterium exchange gives us the symmetry properties of ψ_{ex}, antisymmetric for the lower state and symmetric for the upper. This agrees with the finding for the hfs in Ar_2-H_2O as summarized in Table VII, which has the same symmetry as the $Ar-H_2O/D_2O$ dimer.[4]

The physical process responsible for ψ_{ex} remains to be examined more carefully. The two most likely candidates are tunneling or internal rotor states of the H_2O/D_2O, the latter proposed by Cohen and Saykally[1] to account for the two sets of rotational transitions found for the $Ar-H_2O/D_2O$ dimer. In their internal rotor model the H_2O/D_2O is virtually free to rotate and ψ_{ex} for the lower state corresponds to the antisymmetric 1_{01} state of free H_2O, while the upper state corresponds to the symmetric 0_{00} state.

In the preliminary account of $Ar_m-(H_2O)_n$ clusters[5] we were impressed by the similarities between Ar_2-H_2O and the behavior reported previously for the pseudolinear Ar_2-H_2O dimer. This led us to attribute without qualification the two sets of transitions for Ar_2-H_2O to the two sets of H_2O internal rotor states used so successfully for Ar_2-H_2O. However, subsequent MMC calculations[19] gave the planar equilibrium structure of Fig. 1. Its bidentate form seemed likely to inhibit free rotation of the H_2O/D_2O and encouraged the following more extensive analysis of the energy surface via the MMC model.[14]

MMC CALCULATIONS

The potential in the MMC model is based on a combination of classical electrostatic interaction energies, including mutual polarization and hyperpolarization, with energy terms designed to represent the nonelectrical contributions in the form of atom–atom Lennard-Jones potentials. The values

TABLE V. ^{17}O hyperfine structure of the $J=0_{00}+1_{11}$ transitions for $Ar_2-H_2\ ^{17}O$.

	Lower state		Upper state	
$F\rightarrow F'$	Observed (MHz)	Residue (kHz)	Observed (MHz)	Residue (kHz)
5/2→5/2	4356.5045	0.0	4437.9801	0.2
5/2→7/2	4357.3760	0.0	4438.2612	−0.7
5/2→3/2	4357.7495	0.0	4438.3834	0.5
Line center	4357.1685		4438.1948	
χ_{bb}	4.15		1.343	

TABLE VI. Comparison of D and ^{17}O quadrupole interaction constants determined from the hfs of the $0_{00}\rightarrow 1_{11}$ transitions for the lower and upper states of isotopomers of the dimer and trimer.

Isotopomer	Interaction	Lower state (MHz)	Upper state (MHz)
Ar–D_2O[a]	χ_{aa}(D)	0.083	0.119
Ar_2–D_2O	χ_{bb}(D)	0.083	0.125
Ar–H_2 ^{17}O[b]	$\chi_{aa}(^{17}O)$	4.22	1.23
Ar_2–H_2 ^{17}O	$\chi_{bb}(^{17}O)$	4.15	1.343

[a]From Ref. 4.
[b]From Ref. 3.

of electrical properties in the potential are from *ab initio* calculations whereas the parameters in the Lennard-Jones terms are empirical. All are associated with individual molecules, in this case an argon atom and a water molecule, and are transferable from one complex to another. That is, no adjustment of the parameters[14] has been made for the complex studied here.

The MMC model tends to be more complete in representing electrical interaction than nonelectrical interaction. Clusters with rare gas atoms tend to have relatively smaller electrical interaction energies contributing to their stabilities than do clusters of molecules possessing nonvanishing charge fields. Therefore, the argon–water interaction approaches the limit of applicability of the MMC model. For instance, Bacic's dynamical analysis[20] of a similar dimer, Ar–HCN, using the MMC potential gave reasonable results but not quantitative values of the vibrational transition frequencies. Error in the nonelectrical representation will certainly affect the predicted molecule–rare gas separation distance.

At the same time, the overall shapes and features of molecule-rare gas MMC potentials (troughs, location of minima, etc.) have been reliable. The argon–argon pair potential is well-represented in MMC with a ''6–12'' potential, and three-body effects for Ar_2–H_2O are developed in the potential via the polarization energetics. Thus, we expect the model to be especially useful here in showing how the potential surface affects rotation of the water from its equilibrium orientation and how the H_2O changes the Ar–Ar interaction.

The equilibrium structure found for Ar_2–H_2O is that shown in Fig. 1. The heavy atoms are in a T shape with each hydrogen pointed at one of the argons in a bidentate bond. The overall structure is planar with C_{2v} symmetry. The stabilities and inter-c.m. distances are given in Table VIII for the Ar–Ar and Ar–H_2O dimers and the Ar_2–H_2O trimer. If there were no three-body effects $D_e(Ar_2–H_2O)$ would equal $D_e(Ar–Ar)+2D_e(Ar–H_2O)$. However the sum is -557.2 cm^{-1} while the direct MMC value is only -550.1 cm^{-1}, indicating that the trimer is 7.1 cm^{-1} less stable than if there were no three-body effects. The difference is small but it seems likely to be real. Apparently, in the trimer the H_2O cannot simultaneously be at the optimum Ar–H–O angle for both hydrogens. The Ar_2 tries to help out by stretching from 3.760 to 3.774 Å but the net effect is a slightly less stable trimer.

TABLE VII. Symmetry conditions on exchange of protons or of deuterons in the lower and upper states of Ar_2–H_2O/D_2O.

		Ar_2–H_2O		Ar_2–D_2O	
Function	Source	Lower	Upper	Lower	Upper
χ_{nuc}	Observed	sym. (I_H=1)	antisym. (I_H=0)	antisym. (I_D=1)	sym. (I_D=0,2)
χ_{ex}	Predicted	antisym.	sym.	antisym.	sym.
χ_T	Required	antisym.	antisym.	sym.	sym.

TABLE VIII. Dimer and trimer equilibrium stabilities, dissociation energies, and center of mass separations calculated with the MMC model for Ar_2–H_2O.

Cluster	D_e (cm^{-1})	D_0 (cm^{-1})	r(Ar–Ar) (Å)	R(Ar–H_2O) (Å)
Ar–Ar	−96.6	−82	3.760	⋯
Ar–H_2O	−230.3	−131	⋯	3.410
Ar_2–H_2O	−550.1	−364	3.774	3.407

A clarifying presentation of the full PES is difficult even though the trimer is quite symmetric. After allowing for the symmetry there are still five internal coordinates to consider—three rotational angles for a rigid H_2O, the Ar to Ar distance r and the c.m. (Ar_2) to c.m. (H_2O) distance R. An overall view of the PES is given in Fig. 2 which is a contour plot of the potential energy as a function of the relative positions of H_2O and Ar_2. The plot is for the x,y plane with the c.m. (H_2O) at x,y grid points. The Ar_2 is on the x axis, centered at the origin. For each x,y grid point the potential was optimized by adjusting r and the H_2O orientation (not shown). The optimized structures are planar. There is a mirror image at $-y$.

The rotational freedom of the H_2O is given by its change in potential energy over the rotational path. For tunneling exchange of the water protons, the water needs to rotate 180° about its C_2 axis. This corresponds to the b inertial axis of the water and to θ_b as shown in Fig. 1. The MMC potential

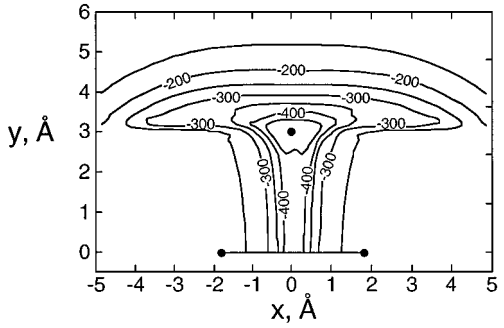

FIG. 2. Contour plot of the MMC potential energy surface for the Ar_2–H_2O trimer. The dots are the equilibrium positions of the argons and the H_2O c.m. The Ar_2 is on the x axis, centered at the origin. The potential was optimized at each x,y grid point by adjusting r and the H_2O orientation. The resulting surface is planar.

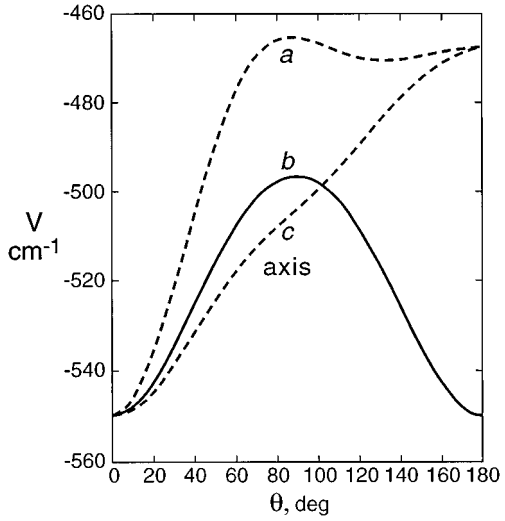

FIG. 3. Potential energy curves for the rotation of H_2O about its *a*, *b*, or *c* axis in the Ar_2–H_2O trimer. At each point on a curve both *r* and *R* were relaxed (optimized).

for the path is given in Fig. 3. The path starts at the planar equilibrium structure and the potential is optimized for each θ_b by relaxing both *r* and *R*. The resulting path has a sin-shaped barrier of 54 cm^{-1}. In addition, Fig. 3 includes potential curves for rotation of the water about its *a* axis and *c* axis both of which have higher predicted barriers of about 80 cm^{-1}.

Taken alone, these results would favor tunneling exchange as the mechanism splitting the rotational states of Ar_2–H_2O/D_2O. However, strong rovibrational coupling in the right modes can enable the zero-point energy to surmount the barrier. An estimate of the zero-point modes of a cluster may be obtained from the MMC model potential by evaluating the force constants for the intermolecular degrees of freedom (i.e., with fixed monomer structures). Harmonic vibrational frequencies of the weak bonding modes are calculated using the force constants.[21] Then the zero-point energy estimate is taken to be one-half of the sum of these frequencies. The true zero-point energies of clusters tend to be less than the harmonic evaluation, probably by 5%–20%. The MMC calculations on Ar_2–H_2O give harmonic frequencies ranging from 26 to 118 cm^{-1}, as listed in Table IX. The lowest frequency (26 cm^{-1}) is the Ar–Ar stretching mode and the highest (118 cm^{-1}) is the water torsion about its *a*-axis, with a total harmonic zero-point energy of 186 cm^{-1}. Thereby the torsional mobility of the H_2O appears to be high enough to allow the internal rotor states observed.

TABLE IX. Weak vibrational modes of Ar_2–H_2O and their harmonic frequencies and doubly harmonic transition moments calculated from the MMC potential.

Vibrational mode	Frequency (cm^{-1})	Transition moment (D)
Ar–Ar stretch	26	0.0043
Water torsion about its *b* axis	43	0.83
Pyramidal motion or puckering	53	0.10
Water torsion about its *c* axis	61	0.002
Water to Ar_2 stretch	70	0.028
Water torsion about its *a* axis	118	0.78

The MMC model potential involves solving mutual polarization equations for the interacting species in a cluster so an automatic result is the enhancement in the dipole moment arising from polarization. For Ar_2–H_2O, the enhancement at the MMC equilibrium structure is found to be 0.28 D. The dipole moment information generated via MMC means that the dipole moment surface of the cluster is calculable. From this, one may obtain the derivatives of the dipole moment with respect to displacement coordinates. The first derivatives with respect to the weak-mode normal coordinates are the so-called doubly harmonic vibrational transition moments. Though harmonic frequencies are not likely to serve as a good predictor of the ir spectrum of the cluster, the calculated intensities show differences that may be of qualitative value for studying the spectrum. Table IX includes the transition moments we have found in this manner.

DYNAMIC STRUCTURE

Several features of the Ar_2–H_2O trimer support the conclusion that the spectral doubling is caused by internal rotor states and not by tunneling. The most direct evidence is probably the nonequality of $\chi_{bb}(D)$ in the lower and upper states of Ar_2–D_2O. The hfs in Table IV for Ar_2–D_2O, neglecting spin rotation, gives $\chi_{bb}(D)$ to be 83 kHz for the lower state and 132 for the upper. However, as found for the DF dimer,[22,23] tunneling interchanges of the two *D*'s would average their interactions in the two states, giving the same $\chi_{bb}(D)$. Also, the effects of deuterium substitution on the rotational constants in Table III are unusual and hardly consistent with tunneling. The *A*, *B*, and *C* rotational constants for the two states of Ar_2–H_2O differ by 94, −3, and 15 MHz while those for Ar_2–D_2O differ by 60, −3, and 15 MHz. For a tunneling mechanism one would expect deuterium substitution to have a good deal larger affect on all of the differences rather than a modest 35% decrease in ΔA alone. There is also the observation made earlier[5] that D_2O substitution has virtually no effect on *B* for either the lower or upper state.

In fact the five upper state *B*'s in Table III are virtually identical at 1731.16 to 1731.78 MHz while the two lower states have *B*'s of 1734.65 and 1734.14 MHz. The values for the upper states bracket closely the *B* for the free Ar_2 dimer,[16] implying that the water does not contribute to *B* in the trimer. This is plausible if the water undergoes ''free'' internal rotation with little or no coupling of its internal angular momentum to the inertial frame of the trimer. Such coupling would be smallest for the 0_{00} spherically symmetric internal rotor state as is indeed found for the upper states. On the other hand *B* is *increased* by 3.5 MHz when the water is excited to the 1_{01} internal rotor state. This difference in the rovibrational coupling is described via the inertial defects which are large *positive* quantities, 3.52 and 6.73 $\mu Å^2$ for upper (0_{00}) and lower (1_{01}) states.

Another intriguing aspect of our study is finding the hf interaction constants of the water in Ar_2–H_2O/D_2O to be very nearly the same as those for the dimer Ar–H_2O/D_2O (Table VI). The observed constants are related to the coupling constant in free water by projecting the coupling onto the dipolar inertial axis of the complex and averaging over the dynamic state of the water.[4] The projection axis is the *b* axis for the trimer and the *a* axis for the dimer, which have equivalent symmetry. The close similarity in the hf constants shows the two dynamic states of the water to be the same in the dimer and trimer, as is the average orientation of the water C_2 axis with respect to the inertial axis.

These observations show that the upper states of the trimers are perturbed least. On this basis we use the rotational constants for the upper state of Ar_2–H_2O to estimate the structural dimensions of the trimer. In this case the following inertial equations apply:

$$I_a = \mu_c R^2, \tag{1}$$

$$I_b = I(\mathrm{Ar}_2) = \tfrac{1}{2} m r^2, \tag{2}$$

$$I_c = \tfrac{1}{2} m r^2 + \mu_c R^2. \tag{3}$$

Here μ_c is the reduced mass of the cluster treated as pseudodiatomic, m is the mass of Ar, r is the Ar–Ar distance, and R is the cm-to-cm distance between Ar_2 and H_2O. Equation 2 leads to an r value of 3.822 Å, which is virtually identical to that observed in the free dimer, 3.821 Å. Equations (1) and (3) lead to R values of 3.154 and 3.191 Å, respectively. These values correspond to Ar-c.m.(H_2O) distances of 3.687 and 3.720 Å, which closely bracket that found in the Ar–H_2O dimer, 3.691 Å. As expected, the MMC results for the equilibrium values of r and R are considerably smaller (3.774 and 2.964 Å) than the observed effective distances.

ACKNOWLEDGMENTS

This report is based upon work supported by the Physical Chemistry Division of the National Science Foundation under Grants CHE 91-17199 and 94-13380 to H.S.G. and CHE 94-03545 to C.E.D. We thank G. T. Fraser for encouragement and assistance.

[1] R. C. Cohen and R. J. Saykally, J. Chem. Phys. **98**, 6007 (1993), and references therein.
[2] D. J. Nesbit and R. Lascola, J. Chem. Phys. **97**, 8096 (1992).
[3] G. T. Fraser, F. J. Lovas, R. D. Suenram, and K. J. Matsumura, J. Mol. Spectrosc. **144**, 97 (1990).
[4] T. C. Germann and H. S. Gutowsky, J. Chem. Phys. **98**, 5235 (1993).
[5] E. Arunan, T. Emilsson, and H. S. Gutowsky, J. Am. Chem. Soc. **116**, 8418 (1994).
[6] A. Ben-Naim, J. Chem. Phys. **90**, 7412 (1989), and references therein.
[7] H. C. Anderson and K. Watanabe, J. Phys. Chem. **90**, 795 (1986).
[8] D. C. Rapaport and H. A. Scheraga, J. Phys. Chem. **86**, 873 (1982).
[9] L. R. Pratt and D. Chandler, Chem. Phys. **73**, 3430 and 3434 (1980).
[10] H. S. Gutowsky, T. D. Klots, C. Chuang, C. A. Schmuttenmaer, and T. Emilsson, J. Chem. Phys. **83**, 4817 (1985); **86**, 569 (1987).
[11] T. J. Balle and W. H. Flygare, Rev. Sci. Instrum. **52**, 33 (1981).
[12] E. J. Cambell, W. G. Read, and J. A. Shea, Chem. Phys. Lett. **94**, 69 (1983).
[13] See, e.g., C. Chuang, C. J. Hawley, T. Emilsson, and H. S. Gutowsky, Rev. Sci. Instrum. **61**, 1629 (1990).
[14] C. E. Dykstra, J. Am. Chem. Soc. **111**, 6168 (1989); **112**, 7540 (1990).
[15] H. S. Gutowsky, C. Chuang, T. D. Klots, T. Emilsson, R. S. Ruoff, and K. R. Krause, J. Chem. Phys. **88**, 2919 (1988), and references therein.
[16] E. A. Colbourn and A. E. Douglas, J. Chem. Phys. **65**, 1741 (1976); P. R. Herman, P. E. LaRocque, and B. P. Stoichoff, *ibid.* **89**, 4535 (1988).
[17] W. Gordy and R. L. Cook, *Microwave Molecular Spectra* (Wiley, New York, 1984).
[18] J. K. G. Watson, in *Vibrational Spectra and Structure*, edited by J. R. Durig (Elsevier, Amsterdam, 1977), Vol. 6, p. 1. We thank G. T. Fraser for providing us with the NIST program of A. G. Maki used for the fitting.
[19] C. E. Dykstra (unpublished).
[20] M. Mladenovic and Z. Bacic, J. Chem. Phys. **94**, 4988 (1991).
[21] C. E. Dykstra, J. Phys. Chem. **94**, 180 (1990).
[22] B. J. Howard, T. R. Dyke, and W. Klemperer, J. Chem. Phys. **81**, 5417 (1984).
[23] H. S. Gutowsky, C. Chuang, J. D. Keen, T. D. Klots, and T. Emilsson, J. Chem. Phys. **83**, 2070 (1985).